Intracellular estrogen receptor-binding fragment-associated antigen 9 exerts *in vivo* tumor-promoting effects via its coiled-coil region

YOSHIHIRO MAEYAMA[1,2], MAKOTO OTSU[3], SHUJI KUBO[4], TOMOKI YAMANO[5], YASUAKI IIMURA[1,2], MASAFUMI ONODERA[6], SATOSHI KONDO[2], YUKIO SAKIYAMA[1] and TADASHI ARIGA[1,7]

[1]Group of Human Gene Therapy, [2]Department of Surgical Oncology, Hokkaido University Graduate School of Medicine, N15W7 Sapporo, Hokkaido 060-8638; [3]Division of Stem Cell Therapy, Center for Stem Cell Biology and Regenerative Medicine, The Institute of Medical Science, The University of Tokyo, 4-6-1 Shirokanedai, Minato-ku, Tokyo 108-8639; [4]Department of Genetics and [5]Division of Lower Gastrointestinal Surgery, Department of Surgery, Hyogo College of Medicine, 1-1 Mukogawa-cho, Nishinomiya, Hyogo 663-8501; [6]Department of Human Genetics, National Center for Child Health and Development, 2-10-1 Okura, Setagaya-ku, Tokyo 157-8535; [7]Department of Pediatrics, Hokkaido University Graduate School of Medicine, N15W7 Sapporo, Hokkaido 060-8638, Japan

Received February 22, 2011; Accepted April 6, 2011

DOI: 10.3892/ijo.2011.1026

Abstract. Estrogen receptor-binding fragment-associated antigen 9 (EBAG9) is a tumor-promoting factor of largely unknown function. To assess a causative role of EBAG9 in advanced malignancies, we generated the EG7-OVA and MethA murine tumor cell lines that stably express full-length or truncated EBAG9 protein, using retroviral-mediated gene transduction. Upon subcutaneous inoculation into immuno-competent mice, both cell lines showed marked acceleration of *in vivo* tumor growth when full-length EBAG9 was over-expressed. Interestingly, deletion of the coiled-coil region, thereby producing truncated EBAG9 protein, abolished the tumor-acceleration effect, establishing the importance of this domain in EBAG9-mediated tumor promotion. However, there was no alteration in *in vitro* cell proliferation or expression levels of MHC class I and co-stimulatory molecules believed to play a role in immune evasion of tumor cells in these tumor cell lines expressing full-length or truncated EBAG9 protein. Furthermore, both full-length and truncated EBAG9 proteins showed a predominantly cytoplasmic localization in the tumor cells. Collectively, these results suggest that EBAG9 overexpression can be causative in enhancing the malignant properties of tumor cells, and that tumor promotion likely requires EBAG9 intracellular association with as yet unidentified binding partners via the coiled-coil region.

Correspondence to: Dr Tadashi Ariga, Department of Pediatrics, Hokkaido University Graduate School of Medicine, N15W7 Sapporo, Hokkaido 060-8638, Japan
E-mail: tada-ari@med.hokudai.ac.jp

Dr Shuji Kubo, Department of Genetics, Hyogo College of Medicine, 1-1 Mukogawa-cho, Nishinomiya, Hyogo 663-8501, Japan
E-mail: s-kubo@hyo-med.ac.jp

Key words: estrogen receptor-binding fragment-associated antigen 9, tumor promotion, coiled-coil region

Introduction

Identification of the molecules responsible for the development and/or progression of certain malignant tumors has marked significant progress in clinical cancer research, as such molecules serve as prognostic markers and/or therapeutic targets. Recently, estrogen receptor-binding fragment-associated antigen 9 (EBAG9) has come under scrutiny (1). EBAG9 is a ubiquitously expressed protein encoded by an estrogen-responsive gene (1). Studies have suggested that EBAG9 is linked to advanced malignancies, although its function remains undetermined (2-5). Nakashima *et al* (6) demonstrated that EBAG9 was a type II membrane protein that had a C-terminal coiled-coil region at the cell surface that could bind to the putative receptor in T cells and NK cells, thereby inducing their apoptotic cell death (6), and named it receptor-binding cancer antigen expressed on SiSo cells (RCAS1). However, Engelsberg *et al* presented a new finding that EBAG9 was a Golgi-resident protein that modulates cell surface glycosylation by a series of biochemical and cellular imaging analyses (7-11). They proposed that EBAG9-overexpression might contribute to the antigenicity of tumor cells by generation of the tumor-associated *O*-linked glycan Tn antigen (for example, 22.1.1 antigen).

Recently, Ogushi *et al* demonstrated that the overexpression of EBAG9 in a murine renal carcinoma cell line enhanced *in vivo* tumorigenesis, providing the first evidence of a tumor-promoting function for EBAG9 (12). They also suggested the

involvement of an immune-evasion mechanism in the observed effect mediated by EBAG9, but did not describe whether this overexpressed EBAG9 protein was localized on the cell surface or at the Golgi membrane to exert tumor promotion (12).

In the present study, we examined whether overexpression of EBAG9 would promote *in vivo* tumorigenesis in different syngeneic murine tumor models; EG7-OVA (EG7) tumor cells (13) in C57BL/6 mice and MethA cells (14) in BALB/c mice. Here we demonstrated that both cell lines engineered to express full-length EBAG9 protein showed marked acceleration of *in vivo* tumor growth on an immunocompetent background, without alteration in *in vitro* cell proliferation nor induction of the 22.1.1 antigen, which is thought to represent altered cell surface glycosylation induced by EBAG9-overexpression. Of note, deletion of the C-terminal coiled-coil region abolished tumor-promoting effects without altering its subcellular localization. Our data indicate that EBAG9-overexpression plays a causative role in advanced malignancies in an immunocompetent background, and also demonstrate the possibility that the cytoplasmic localization of EBAG9 with an intact C-terminal coding coiled-coil region is a prerequisite for the execution of *in vivo* tumor promotion.

Materials and methods

Cells. EG7 cells are C57BL/6 mouse lymphoma EL4 cell line transfected with ovalbumin (OVA) (13). MethA is a 3-methylcholanthrene-induced fibrosarcoma cell line of BALB/c mouse origin (14). These cell lines and Jurkat human T-cell leukemia cells were maintained in RPMI-1640 (Sigma, St. Louis, MO, USA) with 10% heat-inactivated fetal bovine serum (FBS; Moregate BioTech, Bulimba, Australia), 2 mM L-glutamine (Sigma), 100 U/ml penicillin-G (Sigma), and 100 μg/ml streptomycin (Sigma). The retrovirus packaging cell line, 293GP (15), was maintained in Dulbecco's modified Eagle's medium (DMEM) (Sigma) supplemented with 10% heat-inactivated FBS, 2 mM L-glutamine, 100 U/ml penicillin G, and 100 μg/ml streptomycin sulfate. Cells were cultured in a humidified 5% CO_2 at 37˚C.

Construction and production of retroviral vectors. Full-length and truncated mouse EBAG9 cDNAs (EBAG9-FL and EBAG9-TR, respectively) were obtained by polymerase chain reaction (PCR) amplification using the first-strand DNA prepared from A20 mouse B lymphoma cells as templates. The truncated variants of EBAG9 cDNAs were designed to express EBAG9 protein lacking the C-terminal region (amino acids 179-213) encoding the coiled-coil region (Fig. 1A). The following primers were used for amplifying EBAG9-FL and EBAG9-TR cDNA: forward; 5'-CGTTTTCACCATGGCCATCAC-3', reverse for full-length: 5'-CATAGCCTGTGTTAGGAAAGC-3', reverse for truncated: 5'-CTCAAATTTTCTGCTGCCTCAGCAC-3'.

These EBAG9 cDNAs were cloned into the transfer plasmid of the bicistronic retroviral vector expressing enhanced green fluorescent protein (EGFP) pGCDN IRES/EGFP (GCDN/EGFP for short), a derivative of the GCDNsap that was previously reported (16), generating retroviral vector transfer plasmids; pGCDN/EBAG9-FL and pGCDN/EBAG9-TR.

To produce vesicular stomatitis virus-G (VSV-G)-pseudotyped retroviral particles, packaging cell line 293GP was co-transfected with each transfer plasmid and pcDNA3.1-VSV-G, generating retroviral vector viruses; GCDN/EGFP, GCDN/EBAG9-FL and GCDN/EBAG9-TR. Vector supernatant was collected and subjected to subsequent concentration steps according to previously reported procedures (16).

Retroviral-mediated gene transduction of murine cell lines. EG7 and MethA cells were seeded at $1x10^5$ cells/well in 6-well plates and transduced by the addition of 50 μl of concentrated retroviral supernatant, followed by centrifugation at 2,000 rpm for 30 min at 32˚C. Cells were cultured for 24 h at 37˚C, and medium containing viral particles was replaced with fresh culture medium. Transduction efficiency was assessed 48-72 h later by determining the percentages of EGFP-positive cells using a FACSCalibur and the CellQuest software (Becton-Dickinson, San Jose, CA, USA). Transduction efficiencies commonly ranged between 20-80%. EG7 and MethA cells were sorted for an EGFP-positive population using a FACS Vantage Cell Sorter (Becton-Dickinson) (17).

Reverse transcription (RT)-PCR analysis. Total RNA samples were prepared from cells using the TRIzol reagent (Invitrogen, Carlsbad, CA, USA), followed by first-strand DNA synthesis using the SuperScript II kit (Invitrogen). Equal amounts of first-strand DNA were added to a mixture of 0.2 μM dNTP, 2.5 U Takara Taq DNA polymerase, 1X PCR buffer (Takara Bio, Otsu, Japan), and 0.4 μM each primer. The PCR consisted of 24 and 28 cycles (94˚C for 30 sec 58˚C for 30 sec, and 72˚C for 30 sec), respectively, for amplification of EBAG9 and glyceraldehyde-3-phosphate dehydrogenase (GAPDH). The following primers were used for PCR amplification: EBAG9-forward (P1): 5'-TTGTACCTGCCTAGCAACAG-3', EBAG9-reverse (P2): 5'-AATTCAATGGTTCTCTCTTC-3', GAPDH-forward: 5'-TATTGGGCGCCTGGTCAC-3',GAPDH-reverse: 5'-AGATGATGACCCTTTTGGCTC-3'. The amplified products were separated on a 1.5% agarose gel and then visualized by UV light.

Cell proliferation assay. EG7 or MethA cells ($1x10^4$ cells/well) were seeded in 96-well flat-bottom plates and then cultured for 48 h. The extent of cell proliferation was assessed using the Cell Proliferation Kit I (Roche Diagnostics, Indianapolis, IN, USA), which utilizes 3-(4,5-dimethyl-2-thiazolyl)-2,5-dipenyl-2H-tetrazolium bromide (MTT) as an indicator of metabolic activity of viable cells, according to the manufacturer's instructions.

In vivo experiments. All procedures involving animals were approved by and performed according to guidelines of the Institutional Animal Care and Use Committee of Hokkaido University Graduate School of Medicine. Female C57BL/6 ($H\text{-}2^b$) and BALB/c ($H\text{-}2^d$) mice (5-8 week of age; CLEA Japan, Tokyo, Japan) were injected s.c. into the abdominal flank of unconditioned mice with $2.5x10^6$ tumor cells that was untransduced or transduced with vectors carrying EGFP, EBAG9-FL or EBAG9-TR (n=6 in each group). Tumors were measured three times per week, and tumor volumes were calculated as $a \times b^2 \times 0.5$ (a, large diameter; b, small diameter). The following

criteria were established to determine when an animal's health was so poor that it needed to be euthanized: in order, paleness of the paws and muzzle, weight loss, lethargy/cachexia, and finally hypothermia, they were necropsied. All remaining mice were euthanized at day 40.

Flow cytometry analysis. A flow cytometer (FACSCalibur) with CellQuest analysis software was used for analyses. Staining involved $1x10^6$ cells incubated with primary monoclonal antibodies, washed with PBS/2% FBS, and secondary antibodies added. After the second incubation, cells were washed and resuspended in PBS/2% FBS for flow cytometry analysis. The antibodies used were anti-EBAG9 mAb clone 5E4 (Oncogene Research Products, San Diego, CA, USA) (isotype control; mouse IgG_1, BD Pharmingen, San Diego, CA, USA), anti-RCAS1 mAb clone 22.1.1 (18) (kindly provided by T. Watanabe and M. Nakashima, and also purchased from MBL, Nagoya, Japan) (isotype control; mouse IgM, BD Pharmingen), phycoerythrin (PE) conjugated anti-H-$2K^b$ mAb clone AF6-88.5 (BD Pharmingen) (isotype control; PE-conjugated mouse IgG_{2a}, BD Pharmingen), biotin-anti-B7-H1 mAb clone 1-111A (eBioscience, San Diego, CA, USA) (isotype control; mouse IgG_{2a}, BD Pharmingen), biotin anti-B7-H4 mAb clone 9 (eBioscience) (isotype control; mouse $IgG_1\kappa$, BD Pharmingen), PE-conjugated rat anti-mouse IgM (BD Pharmingen), R-PE-conjugated rat anti-mouse immunoglobulin (Dako, Kyoto, Japan) and PE-streptavidin (BD Pharmingen). To stain the EBAG9 polypeptides residing intracellularly, cells were treated with the Cytofix/Cytoperm reagent (BD Pharmingen) according to the manufacturer's instructions and stained as described above. For the analysis of H-$2K^b$ in EG7 cells by flow cytometry, cells were assessed 48 h after retroviral-mediated gene transduction.

Immunofluorescence and confocal microscopy. To stain intracellular EBAG9 poly-peptide, MethA and Jurkat cells ($1x10^6$) were fixed, permeabilized (Cytofix/Cytoperm, BD Pharmingen) according to the manufacturer's instructions, then incubated with anti-EBAG9 mAb clone 5E4, washed with PBS/2% FBS, and finally stained with PE-conjugated rat anti-mouse IgG_1 (BD Pharmingen) antibody. To stain the cell surface 22.1.1, $1x10^6$ MethA and Jurkat cells were incubated with anti-RCAS1 mAb clone 22.1.1, washed with PBS/2% FBS, and then stained with PE-conjugated rat anti-mouse IgM (BD Pharmingen) antibody. Nuclei were counterstained with 4',6-diamidino-2-phenylindole (DAPI) (Dojindo Laboratories, Kumamoto, Japan). After staining, cells were put on glass slides, scanned and digitized using a confocal laser scanning microscope (Leica TCS SP2, Wetzlar, Germany) with a 63x/1.40 NA oil-immersion objective (Leica). Images were assembled with Adobe Photoshop (Adobe Systems, San Jose, CA, USA).

Western blot analysis. To assess the expression levels of actin and OVA, Western blot analysis was performed following previously described procedures (17). Briefly, cell lysates (50 μg) were first separated on a 4-20% gradient polyacrylamide gel (Daiichi Pure Chemicals Co., Ltd., Tokyo, Japan). After electrotransfer onto a PVDF membrane, OVA protein and actin were respectively reacted with anti-chicken egg albumin mAb (clone OVA-14; Sigma) and anti-actin mAb (clone C-2; Santa Cruz Biotechnology, Inc., Santa Cruz, CA, USA). All the above mAbs are of mouse IgG1-isotype. Following the reaction with horseradish peroxidase-bovine anti-mouse IgG (Santa Cruz), each band was visualized using the ECL system (Amersham Pharmacia Biotech, Inc., Piscataway, NJ, USA). Western blot analyses were quantified by densitometry using Image J 1.43 (National Institute of Health, Bethesda, MD, USA).

Inhibition of T cell proliferation. EG7 or MethA cells were seeded at $1x10^6$ cells/well in 6-well plates. After 48 h, supernatant was collected and used after filtration through 0.45 μm filters. Splenocytes obtained from C57BL/6 mice were stimulated with anti-CD3 mAb (10 ng/ml, BD Pharmingen) in the presence of interleukin-2 (50 U/ml) at $1x10^5$ cells/well in 96-well flat-bottom plates. Graded doses of the above supernatant samples were included in each well to assess their inhibitory effects on T cell proliferation. On day 3, the extent of T cell growth was determined using Cell Counting Kit-8 (Dojindo Laboratories), according to the manufacturer's instructions.

Statistical analysis. The results are presented as the mean ± standard deviation (SD) or standard error of the mean (SEM). Statistical significance of differences was calculated using one-way ANOVA followed by Tukey's test, and a $P<0.01$ was considered significant in all analyses. Tumor volumes were compared by Kruskal-Wallis ANOVA, followed by *post hoc* comparisons with Dunn's test (intergroup comparison).

Results

Generation of EBAG9-expressing murine tumor cell lines. To test whether overexpression of EBAG9 enhanced the malignant properties of tumor cells, we constructed the retroviral vectors GCDN/EBAG9-FL and GCDN/EBAG9-TR to express full-length- or truncated-EBAG9 protein, together with the EGFP in transduced cells (Fig. 1A). We have prepared EBAG9-FL and EBAG9-TR, as well as a control vector, GCDN/EGFP, harboring only EGFP cDNA (Fig. 1A).

We next transduced the well-characterized murine tumor cell lines, EG7 (13) and MethA (14), with the vectors expressing either EBAG9-FL or EBAG9-TR. After sorting the EGFP positive population to enrich EBAG9 transgene-positive cells, we performed RT-PCR analysis using the primer pair specific for EBAG9 cDNA (P1 and P2, Fig. 1A). As shown in Fig. 1B, we found that minimum levels of endogenous EBAG9 mRNA was expressed in both untransduced EG7 and MethA cells (Fig. 1B, UT). In contrast, enhanced expression of EBAG9 mRNA was evident in both EG7 and MethA cells after transduction with the GCDN/EBAG9-FL or -TR vectors (Fig. 1B). Eventually, EG7 and MethA cell lines were successfully engineered to stably express the full-length or truncated EBAG9 transgene.

In vitro and in vivo growth of the EBAG9-expressing murine tumor cells. To explore whether overexpressed EBAG9 would promote cell proliferation, we performed an MTT-based colorimetric assay. Neither EG7 nor MethA cells exhibited significant acceleration of cell proliferation associated with overexpression of the EBAG9-FL or EBAG9-TR transgene (Fig. 2A), indicating that the forced expression of EBAG9 did not affect *in vitro* cell proliferation.

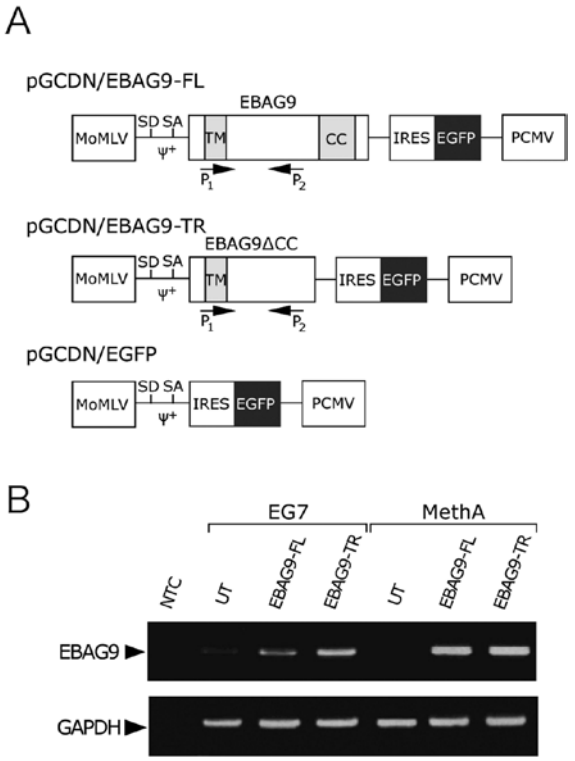

Figure 1. Generation of murine tumor cells stably expressing full-length or truncated EBAG9 using retroviral vectors. (A) Schematic representation of the retroviral constructs. MoMLV, long terminal repeat (LTR) of Moloney murine leukemia virus; y^+, MoMLV packaging signal; SD, splicing donor site; SA, splicing acceptor site; TM, transmembrane region; CC, coiled-coil region; IRES, internal ribosomal entry site; EGFP, enhanced green fluorescent protein; PCMV, LTR of PCC4 cell-passaged myeloproliferative sarcoma virus. Relative location of the primers used for RT-PCR is shown (P1 and P2). During the process of reverse transcription, the 3' PCMV-LTR is used to reconstitute that of the 5' LTR. Therefore, the EBAG9-transgene, either in a full-length (EBAG9-FL) or an EBAG9ΔCC truncated form (EBAG9-TR), is expressed under control of the PCMV enhancer/promoter. (B) RT-PCR analysis of EBAG9 mRNA expression in MethA and EG7 cells. Total RNA was extracted from cells, including untransduced (UT), and transduced cells with full-length or truncated EBAG9. The RNA was reverse-transcribed and amplified by PCR with specific primers for EBAG9 and GAPDH. Intensified signals representing EBAG9- (320 bp) and GAPDH-amplicons (327 bp) are shown. GAPDH was used as an internal control for RT-PCR and blank control was used for negative control (NTC).

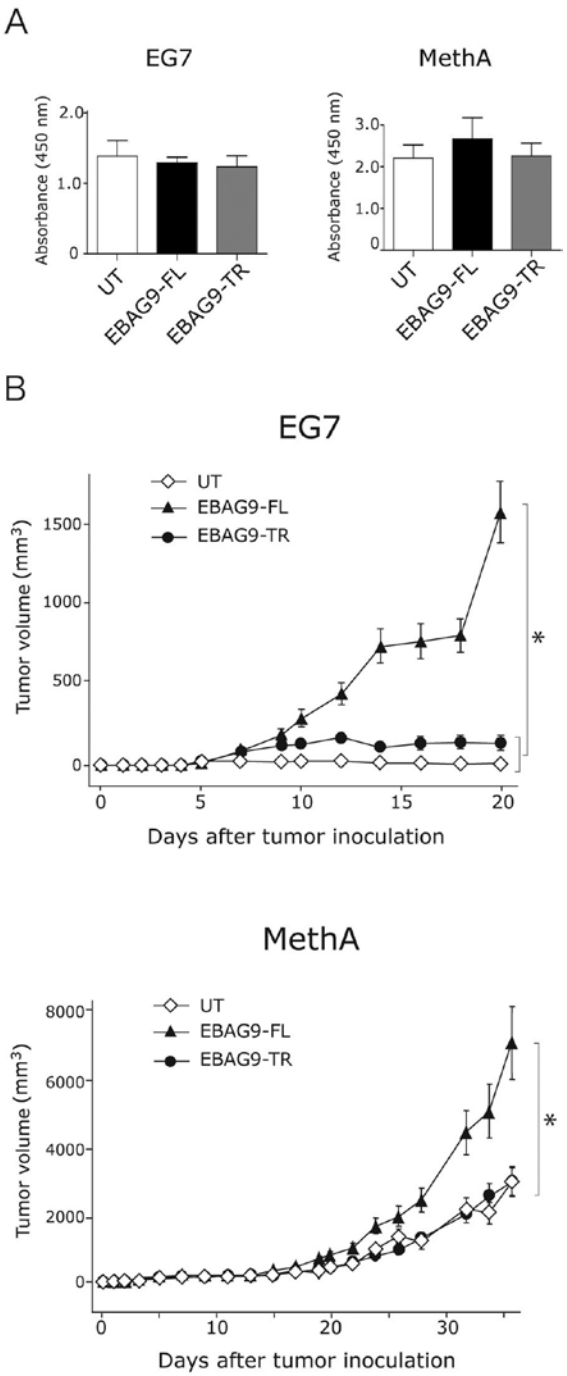

Figure 2. *In vitro* and *in vivo* growth of EBAG9-overexpressing murine tumor cells. (A) *In vitro* growth. EG7 and MethA cells were cultured for 48 h, and cell proliferation was assessed as described in Materials and methods. Values are the means ± SD obtained from triplicate cultures. Representative results from two independent experiments are presented. (B) *In vivo* growth. Tumor growth was monitored after subcutaneous inoculation of the EG7 tumor cells into C57BL/6 mice (top panel) and MethA cells into BALB/c mice (bottom panel). Tumor volumes were measured three times per week and data shown are the means ± SEM (n=6 per group). *P<0.01.

We then investigated the *in vivo* tumor formation and growth of EG7 and MethA cells overexpressing EBAG9 in immunocompetent strains of C57BL/6 and BALB/c mice, respectively. When inoculated with these EG7 cell lines, tumors did not grow in the UT and EBAG9-TR groups (Fig. 2B, upper panel). In the EBAG9-FL group, however, striking acceleration of tumor growth was observed in all inoculated mice (Fig. 2B, upper panel, P<0.01 versus other groups). Similarly, MethA cells overexpressing full-length EBAG9 (EBAG9-FL) exhibited a clear acceleration of *in vivo* tumor growth compared with the other two groups in BALB/c animals (Fig. 2B, lower panel, P<0.01 versus other groups). Collectively, these results demonstrated that these murine tumor cells were able to enhance their malignant properties *in vivo* in immunocompetent animals when engineered to overexpress full-length EBAG9 protein.

Cellular localization of full-length and truncated EBAG9. To investigate the cellular localization of overexpressed EBAG9 protein, we first examined the expression pattern of EBAG9 gene products with or without cell-permeabilization by flow cytometry. Analysis of non-permeabilized EG7 cells revealed cell surface expression of EBAG9 molecules, which was observed at comparable levels to the transduced EG7 cells (Fig. 3A, left panel). Remarkably, analysis of permeabilized

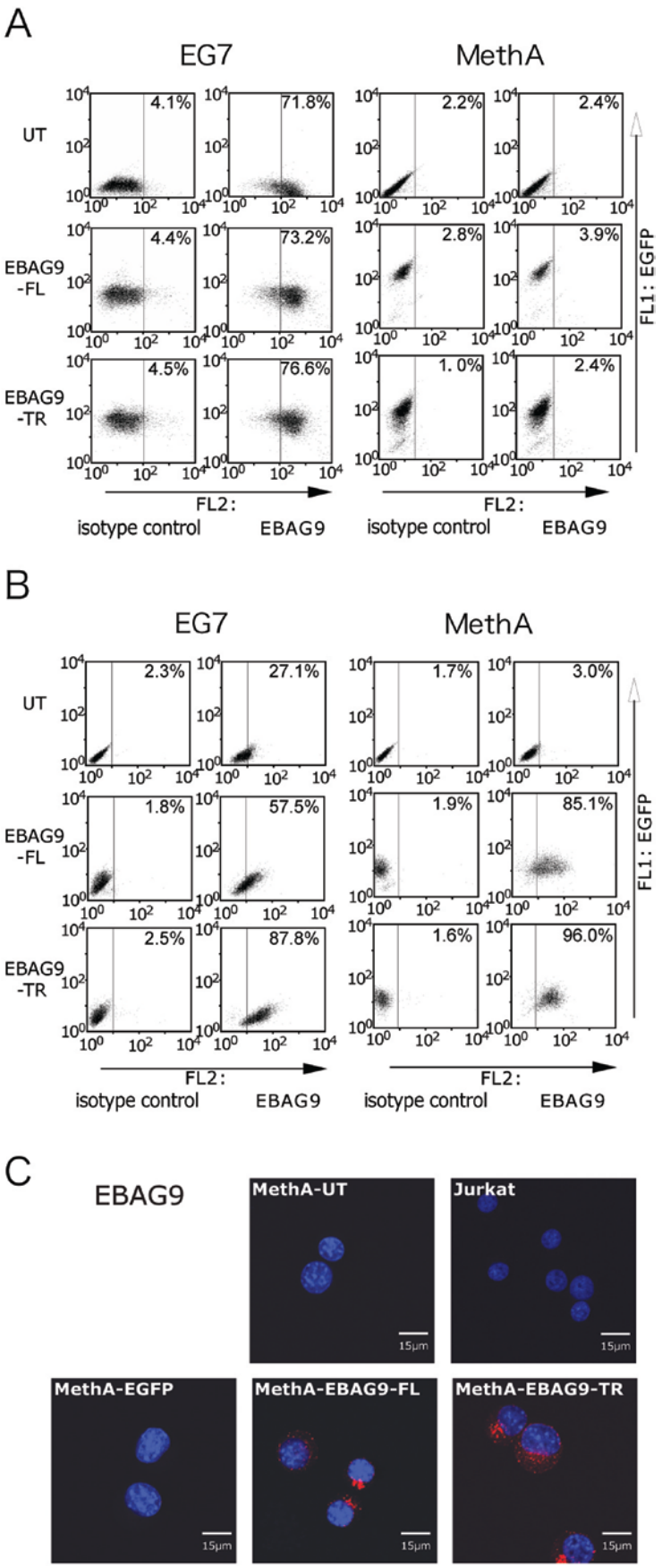

Figure 3. Cellular localization of full-length and truncated EBAG9. (A) Cell surface expression of EBAG9 in EG7 and MethA cells. Unfixed cells were stained with anti-EBAG9 mAb clone 5E4 and PE-conjugated rat anti-mouse IgG1 antibody before expression of EGFP and cell surface EBAG9 was analyzed by flow cytometry. (B) Intracellular expression of EBAG9 in EG7 and MethA cells. Cells were fixed, permeabilized, stained (see Materials and methods) and analyzed. Note the dim EGFP fluorescence intensities caused by the fixation/permeabilization, since GFP accumulates in the cytoplasm and then readily leaks out of permeabilized cells. (C) Confocal microscopic analysis of EBAG9 expression. MethA and Jurkat cells were fixed, permeabilized, and stained with anti-EBAG9 mAb clone 5E4 and PE conjugated rat anti-mouse IgG1 antibody. Shown are EBAG9 in red (PE) and nuclei in blue (DAPI).

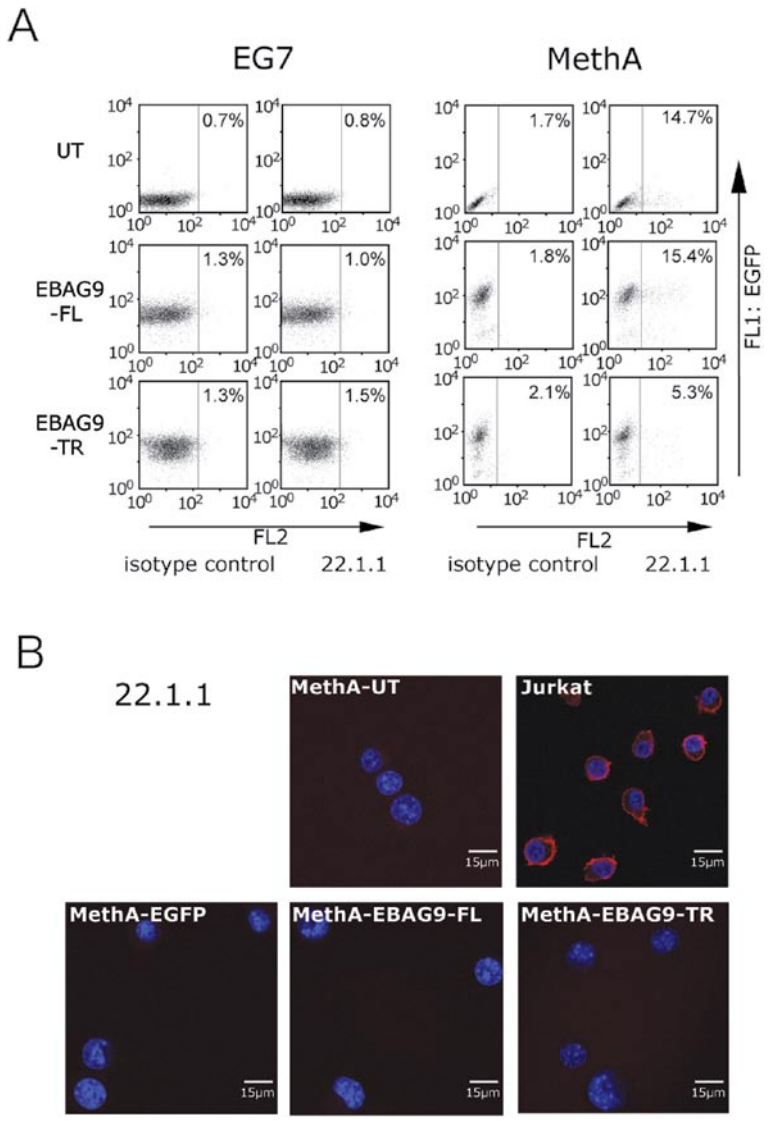

Figure 4. Effect of overexpressed full-length and truncated EBAG9 on 22.1.1 antigen expression. (A) Flow cytometry analysis of cell surface 22.1.1 expression in EG7 and MethA cells with EBAG9-gene transduction. Cell surface expression of 22.1.1 antigen was evaluated by staining unfixed cells with anti-RCAS1 mAb clone 22.1.1 and PE-conjugated rat anti-mouse IgM antibody. (B) Confocal microscopic analysis of cell surface expression of 22.1.1 antigen. MethA and Jurkat cells were stained with anti-RCAS1 mAb clone 22.1.1 and PE-conjugated rat anti-mouse IgM antibody. Shown are the 22.1.1 antigen in red (PE) and nuclei in blue (DAPI).

EG7 cells revealed that the overexpression of both full-length and truncated EBAG9 in EG7 cells enhanced EBAG9 expression in the cytoplasm (Fig. 3B, left panel). In contrast, in MethA cells we detected no EBAG9 staining on the cell surface, despite the presence of the transgene (Fig. 3A, right panel), but enhanced intracellular expression in transduced cells (Fig. 3B, right panel).

To explore the cellular localization of EBAG9-FL, and EBAG9-TR, we performed confocal immunofluorescence microscopy. No EBAG9 labeling was detected at any location in untransduced (MethA-UT and Jurkat) and EGFP-transduced control MethA cells (MethA-EGFP). In the EBAG9-transduced cells, both full-length and truncated EBAG9 proteins were shown to be localized predominantly in an intracellular location (Fig. 3C), which is consistent with the results that were obtained by flow cytometry analysis (Fig. 3A and B).

Taken together, these results suggest that overexpressed full-length and truncated EBAG9 proteins were mainly localized to intracellular compartments in the transduced EG7 and MethA cells, irrespective of their basal expression levels of endogenous EBAG9.

Effect of overexpressed full-length and truncated EBAG9 on cell surface 22.1.1 antigen expression. We next investigated whether EBAG9 overexpression could alter cell surface glycosylation as previously reported (9), using another mAb clone, 22.1.1, which detects the tumor-associated Tn antigen (22.1.1 antigen) induced on the cell surface (9). As shown in Fig. 4A (left panel), no visible 22.1.1-reactivity was observed in EG7 cells, even when transduced with EBAG9-FL and EBAG9-TR. In MethA cells, low-level basal staining was seen in untransduced cells (Fig. 4A, right panel, UT), but enhancement of 22.1.1 reactivity was not apparent in any of the transduced cells (Fig. 4A, EBAG9-FL and -TR).

Confocal immunofluorescence microscopy also revealed that the 22.1.1 antigen was detected only at the cell surface

of untransduced Jurkat cells, but not in any of the MethA cell groups, even when transduced with EBAG9-FL and EBAG9-TR (Fig. 4B).

These results demonstrated that the retroviral-mediated EBAG9 overexpression achieved in this study was not sufficiently high to modify cell surface glycosylation in transduced EG7 and MethA tumor cells, indicating that alteration of cell surface glycosylation may not be the cause for the observed EBAG9-mediated acceleration of *in vivo* tumor growth.

Expressions of OVA, MHC class I, and B7-H1/H4 in tumor cells overexpressing full-length and truncated EBAG9. EG7 cells express OVA protein as a model tumor-associated antigen (TAA) recognizable by immunocompetent hosts. The enhanced *in vivo* tumor growth observed in the EBAG9-FL group suggested the inhibition of immune responses against OVA. At first, we examined the expression levels of OVA in a series of EG7 cells. Western blot analysis showed comparable amounts of OVA protein in all the EG7 cell samples regardless of transgene expression (Fig. 5A).

We next investigated the expression of H-2K^b major histocompatibility complex (MHC) class I that may be involved in immune escape. Similar levels of H-2K^b expression were observed in EGFP-positive (EBAG9-expressing) and EGFP-negative (untransduced) populations in EBAG9-overexpressing EG7 cells (Fig. 5B, EBAG9-FL and -TR). Similarly, the reduction in MHC class I expression was not observed in EBAG9-overexpressing MethA cells (data not shown). These results suggest that the observed EBAG9-mediated acceleration of *in vivo* tumor growth is not attributable to the down-modulation of MHC class I expression and the subsequent reduction in TAA presentation.

We also examined whether the expression of cell surface molecules, which can lead to tumor cell immune evasion, might contribute to the EBAG9-mediated *in vivo* tumor promotion. Therefore, we examined the cell surface expression of B7-H1 and B7-H4, both of which have been recently implicated in cancer immune evasion (19-22). As shown in Fig. 5C, we found that both cell lines similarly expressed B7-H1 on the cell surface (left panel, UT), whereas they did not exhibit any detectable staining of B7-H4 (right panel, UT). In both cases, EBAG9 expression did not induce any alteration in the levels of these molecules (Fig. 5C, EBAG9-FL and -TR), thereby excluding the possibility of B7-H1- or B7-H4-mediated immune evasion as a mechanism of EBAG9's *in vivo* tumor promotion.

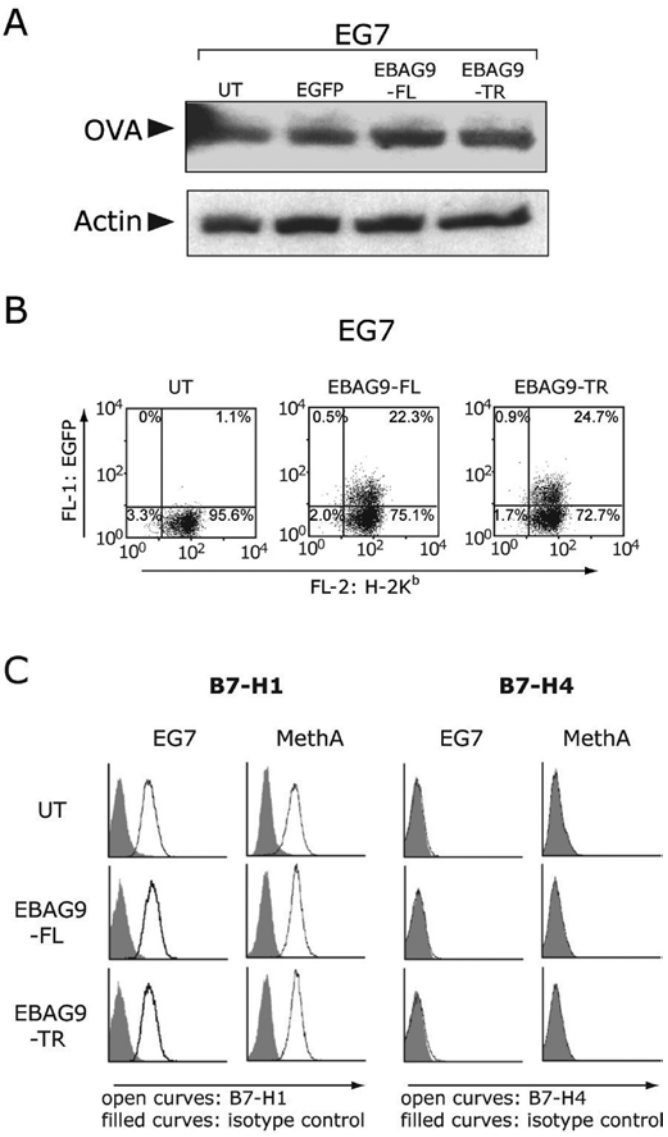

Figure 5. Expressions of OVA, MHC class I, and B7-H1/H4 in tumor cells overexpressing full-length and truncated EBAG9. (A) Western blot analysis of OVA antigen. Protein samples obtained from exponentially growing cells were analyzed with anti-chicken egg albumin mAb. Actin was used as an internal control. (B) Flow cytometry analysis of the expression level of cell surface MHC class I molecule H-2K^b. To enable comparison not only between samples but also within a cell population, unsorted transduced cells (~30% EGFP-positive) were used in this analysis. (C) Flow cytometry analysis of the cell surface B7-H1 and B7-H4. Cells were analyzed by staining with biotin-conjugated anti-B7-H1 or B7-H4 mAb and PE-streptavidin.

Effect of supernatant from murine tumor cells overexpressing full-length and truncated EBAG9 on T cell proliferation. We finally assessed whether EBAG9-overexpression would induce the secretion of any T cell proliferation inhibitory factors from the transduced tumor cells. We prepared filtered supernatant samples from viable cultured tumor cells, and then added them to cultures of anti-CD3 mAb-stimulated splenic T cells at varying doses (Fig. 6). Interestingly, the supernatant obtained from untransduced EG7 cells showed dose-dependent inhibition of T cell proliferation (Fig. 6, upper panel, UT). Overexpression of the full-length- or truncated-version of EBAG9 did not significantly enhance this inhibitory activity (Fig. 6, upper panel, EBAG9-FL and -TR). The supernatant samples obtained from a series of MethA cells did not exhibit significant inhibitory effects on T cell activation, regardless of the presence or absence of overexpressed EBAG9 (Fig. 6, lower panel). These results indicate that EBAG9-overexpression did not lead to the secretion of factors that could lead to detectable levels of inhibition of T cell proliferation in either EG7 or MethA cells.

Discussion

We have demonstrated that overexpression of EBAG9 enhances the *in vivo* malignant properties of murine tumor cells. Although several researchers have suggested a potential link between advanced malignancy and high-level expression of EBAG9 in tumor tissue (3,23-28), evidence that this molecule itself exerts

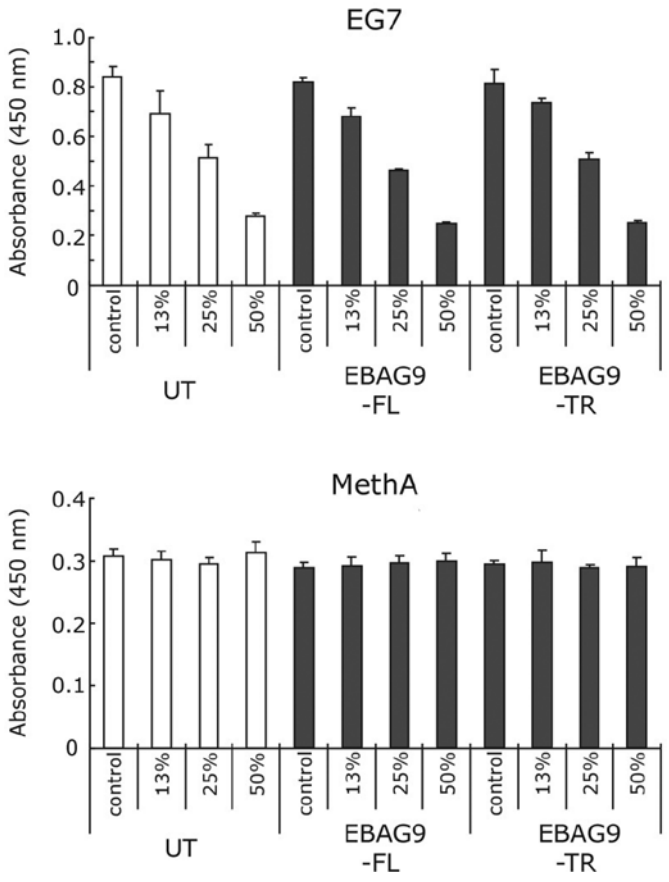

Figure 6. Effect of supernatant from murine tumor cells overexpressing full-length and truncated EBAG9 on T cell proliferation. Culture supernatants obtained from EG7 and MethA cells were collected and added into culture containing stimulated splenocytes from C57BL/6 mice. On day 3, the extent of T cell growth was determined as described in Materials and methods. Data are shown as the means ± SD obtained from triplicate cultures. Representative results from two independent experiments are presented.

an *in vivo* tumor-promoting function has been lacking. Recently, Ogushi *et al* reported for the first time that the enhanced expression of EBAG9 in Renca mouse renal cancer cells leads to accelerated *in vivo* cell growth, using two representative clones generated by transfection of a human EBAG9 cDNA (12). Importantly, they also demonstrated in the same Renca-BALB/c model that the repression of endogenous EBAG9 expression, using RNA interference technology, slows tumor growth (12). Our study has confirmed and extended their observations, as we have demonstrated that retroviral-mediated overexpression of murine EBAG9 accelerates the *in vivo* tumor growth of different tumor cell lines, namely EG7 and MethA. To our knowledge, this is the first study to use retroviral-mediated EBAG9 gene transfer for functional analysis. As the efficient retroviral-mediated transduction eliminated the necessity for cloning procedures, our data are able to reinforce the evidence of the *in vivo* tumor-promoting effects of EBAG9 using uncloned, and thus biologically heterogeneous, cell populations. Moreover, our results added a new notion that both the presence of the coiled-coil region and the intracellular expression of EBAG9 are critical for its *in vivo* tumor-promoting function.

As we and others (12) have now experimentally demonstrated *in vivo* tumor promotion by forced expression of EBAG9, elucidation of the mechanism(s) underlying this observed effect is the obvious next step. Expressed EBAG9 most likely does not directly promote cell proliferation, as we (Fig. 2A) and others (12) did not detect enhancement of *in vitro* cell growth following EBAG9-overexpression. The fact that EBAG9 promotes only *in vivo* tumor growth suggests that overexpression of this molecule likely influences the host environment, including the immune response. Ogushi *et al* demonstrated decreased numbers of $CD8^+$ T cells at the site of growing Renca cells that overexpressed EBAG9 (12). Our results also indicate that immune evasion mechanisms play a role in EBAG9-mediated *in vivo* tumor promotion, as when relatively immunogenic tumor cells, such as EG7 cells, were eradicated, only EBAG9-overexpressing tumors continued to grow in immunocompetent hosts.

The preferential localization of EBAG9 to the Golgi apparatus suggests that the overexpressed protein may modulate cell surface expression of certain molecules that regulate the functions of interacting immune cells. Although alteration of cell surface glycosylation by EBAG9 expression may play a role in enhancing the *in vivo* malignant properties of tumor cells, our results did not support this hypothesis, as the tumor-promoting effects were readily observed in cells that expressed EBAG9 at levels insufficient to induce 22.1.1 antigen expression on the cell surface. Furthermore, EBAG9-overexpressing tumors did not show down-modulation of MHC class I molecules (Fig. 5B), nor enhanced expression of the immune-regulatory molecules, B7-H1 and B7-H4 (Fig. 5C), both of which have recently been implicated in tumor cell immune evasion (19-22). Thus, it is unlikely that EBAG9 exerts its tumor-promoting effects through the modulation of cell surface molecules, although the existence of as yet unidentified targets cannot be excluded.

Finally, altered secretion of soluble factors with immune-regulatory functions may be responsible for the enhanced malignant behavior of tumor cells due to EBAG9-overexpression, as the recent identification of the EBAG9 binding partner, Snapin, suggests a possible role for EBAG9 in regulated secretion pathways (7). However, the supernatant obtained from the culture of tumor cells overexpressing full-length EBAG9 did not show any increased inhibitory effects on T cell proliferation (Fig. 6). These observations indicate that EBAG9-overexpression in our experimental system does not induce the secretion of T cell-inhibitory factors from EG7 and MethA cells to levels where the supernatant would show appreciable inhibition of T cell proliferation. However, the possibility that altered expression of certain immunomodulatory molecules plays a role in EBAG9-mediated enhanced tumori-genesis cannot be completely excluded.

Here we report the importance of the C-terminal coiled-coil region in EBAG9's tumor-promoting function. The mutant we used, which lacks the 35 most-C-terminal amino acids, is predicted to be indistinguishable in biological characteristics from the one (RCAS1Δ179-213-GFP) that Engelsberg *et al* used in their analyses of EBAG9 membrane topology and subcellular localization (9). Considering their results, deletion of the 35 C-terminal amino acids is believed not to affect EBAG9's Golgi-predominant localization, but to abolish the ability to associate with cytoplasmic molecules through the coiled-coil region. As our data support the significance of the coiled-coil region in EBAG9-mediated tumor promotion,

identification of the binding partner will increase our understanding of the underlying mechanism(s). Since the recently identified EBAG9 partner, Snapin, reportedly binds to EBAG9 via the N-terminal region, not the C-terminal coiled-coil domain (7), other molecules that associate with EBAG9's C-terminal region, and thus play a role in *in vivo* tumor-enhancement, may exist.

In vivo tumor promotion is most likely not merely the function of EBAG9, considering a ubiquitous expression pattern (1) and a suggested regulatory role in exocytosis (7) of this molecule. Since our retroviral system allows efficient gene transduction into various primary cells (16,29,30), its broader application in further studies will provide insights into EBAG9's function in many areas, not only tumorigenesis, but also other non-cancerous situations.

Acknowledgments

The authors thank Professor Takeshi Watanabe and Dr Manabu Nakashima (Kyushu University) for the gift of the 22.1.1 mAb. This work was supported in part by Grants-in-Aid for Scientific Research from the Ministry of Health, Labour and Welfare Japan and Ministry of Education, Culture, Sports, Science and Technology Japan.

References

1. Tsuchiya F, Ikeda K, Tsutsumi O, *et al*: Molecular cloning and characterization of mouse EBAG9, homolog of a human cancer associated surface antigen: expression and regulation by estrogen. Biochem Biophys Res Commun 284: 2-10, 2001.
2. Dutsch-Wicherek M, Tomaszewska R, Lazar A, *et al*: The evaluation of metallothionein expression in nasal polyps with respect to immune cell presence and activity. BMC Immunol 11: 10, 2010.
3. Tsuneizumi M, Emi M, Nagai H, *et al*: Overrepresentation of the EBAG9 gene at 8q23 associated with early-stage breast cancers. Clin Cancer Res 7: 3526-3532, 2001.
4. Suzuki T, Inoue S, Kawabata W, *et al*: EBAG9/RCAS1 in human breast carcinoma: a possible factor in endocrine-immune interactions. Br J Cancer 85: 1731-1737, 2001.
5. Aoki T, Inoue S, Imamura H, *et al*: EBAG9/RCAS1 expression in hepatocellular carcinoma: correlation with tumour dedifferentiation and proliferation. Eur J Cancer 39: 1552-1561, 2003.
6. Nakashima M, Sonoda K and Watanabe T: Inhibition of cell growth and induction of apoptotic cell death by the human tumor-associated antigen RCAS1. Nat Med 5: 938-942, 1999.
7. Ruder C, Reimer T, Delgado-Martinez I, *et al*: EBAG9 adds a new layer of control on large dense-core vesicle exocytosis via interaction with Snapin. Mol Biol Cell 16: 1245-1257, 2005.
8. Ruder C, Hopken UE, Wolf J, *et al*: The tumor-associated antigen EBAG9 negatively regulates the cytolytic capacity of mouse $CD8^+$ T cells. J Clin Invest 119: 2184-2203, 2009.
9. Engelsberg A, Hermosilla R, Karsten U, Schulein R, Dorken B and Rehm A: The Golgi protein RCAS1 controls cell surface expression of tumor-associated O-linked glycan antigens. J Biol Chem 278: 22998-23007, 2003.
10. Wolf J, Reimer TA, Schuck S, *et al*: Role of EBAG9 protein in coat protein complex I-dependent glycoprotein maturation and secretion processes in tumor cells. FASEB J 24: 4000-4019, 2010.
11. Reimer TA, Anagnostopoulos I, Erdmann B, *et al*: Reevaluation of the 22-1-1 antibody and its putative antigen, EBAG9/RCAS1, as a tumor marker. BMC Cancer 5: 47, 2005.
12. Ogushi T, Takahashi S, Takeuchi T, *et al*: Estrogen receptor-binding fragment-associated antigen 9 is a tumor-promoting and prognostic factor for renal cell carcinoma. Cancer Res 65: 3700-3706, 2005.
13. Moore MW, Carbone FR and Bevan MJ: Introduction of soluble protein into the class I pathway of antigen processing and presentation. Cell 54: 777-785, 1988.
14. Srivastava PK, DeLeo AB and Old LJ: Tumor rejection antigens of chemically induced sarcomas of inbred mice. Proc Natl Acad Sci USA 83: 3407-3411, 1986.
15. Burns JC, Friedmann T, Driever W, Burrascano M and Yee JK: Vesicular stomatitis virus G glycoprotein pseudotyped retroviral vectors: concentration to very high titer and efficient gene transfer into mammalian and nonmammalian cells. Proc Natl Acad Sci USA 90: 8033-8037, 1993.
16. Suzuki A, Obi K, Urabe T, *et al*: Feasibility of *ex vivo* gene therapy for neurological disorders using the new retroviral vector GCDNsap packaged in the vesicular stomatitis virus G protein. J Neurochem 82: 953-960, 2002.
17. Candotti F, Oakes SA, Johnston JA, Notarangelo LD, O'Shea JJ and Blaese RM: *In vitro* correction of JAK3-deficient severe combined immunodeficiency by retroviral-mediated gene transduction. J Exp Med 183: 2687-2692, 1996.
18. Sonoda K, Nakashima M, Kaku T, Kamura T, Nakano H and Watanabe T: A novel tumor-associated antigen expressed in human uterine and ovarian carcinomas. Cancer 77: 1501-1509, 1996.
19. Dong H and Chen L: B7-H1 pathway and its role in the evasion of tumor immunity. J Mol Med 81: 281-287, 2003.
20. Sica GL, Choi IH, Zhu G, *et al*: B7-H4, a molecule of the B7 family, negatively regulates T cell immunity. Immunity 18: 849-861, 2003.
21. Ichikawa M and Chen L: Role of B7-H1 and B7-H4 molecules in down-regulating effector phase of T-cell immunity: novel cancer escaping mechanisms. Front Biosci 10: 2856-2860, 2005.
22. Dong H, Strome SE, Salomao DR, *et al*: Tumor-associated B7-H1 promotes T-cell apoptosis: a potential mechanism of immune evasion. Nat Med 8: 793-800, 2002.
23. Akahira JI, Aoki M, Suzuki T, *et al*: Expression of EBAG9/RCAS1 is associated with advanced disease in human epithelial ovarian cancer. Br J Cancer 90: 2197-2202, 2004.
24. Brunner M, Erovic B, Heiduschka G, *et al*: RCAS-1 serum and tumor levels in head and neck squamous cell carcinoma. Eur Surg Res 44: 214-219, 2010.
25. Ali-Fehmi R, Chatterjee M, Ionan A, *et al*: Analysis of the expression of human tumor antigens in ovarian cancer tissues. Cancer Biomark 6: 33-48, 2010.
26. Kumagai J, Urano T, Ogushi T, *et al*: EBAG9 is a tumor-promoting and prognostic factor for bladder cancer. Int J Cancer 124: 799-805, 2009.
27. Dutsch-Wicherek M, Tomaszewska R, Lazar A, Wicherek L and Skladzien J: The association between RCAS1 expression in laryngeal and pharyngeal cancer and its healthy stroma with cancer relapse. BMC Cancer 9: 35, 2009.
28. Tsujitani S, Saito H, Oka S, *et al*: Prognostic significance of RCAS1 expression in relation to the infiltration of dendritic cells and lymphocytes in patients with esophageal carcinoma. Dig Dis Sci 52: 549-554, 2007.
29. Nabekura T, Otsu M, Nagasawa T, Nakauchi H and Onodera M: Potent vaccine therapy with dendritic cells genetically modified by the gene-silencing-resistant retroviral vector GCDNsap. Mol Ther 13: 301-309, 2006.
30. Kaneko S, Onodera M, Fujiki Y, Nagasawa T and Nakauchi H: Simplified retroviral vector gcsap with murine stem cell virus long terminal repeat allows high and continued expression of enhanced green fluorescent protein by human hematopoietic progenitors engrafted in nonobese diabetic/severe combined immunodeficient mice. Hum Gene Ther 12: 35-44, 2001.